PHYSICAL REVIEW B VOLUME 44, NUMBER 12 15 SEPTEMBER 1991-II

Hydrogen diffusion and passivation processes in *p*- and *n*-type crystalline silicon

R. Rizk, P. de Mierry, D. Ballutaud, and M. Aucouturier
Laboratoire de Physique des Solide des Bellevue, Centre National de la Recherche Scientifique, 1 place Aristide Briand, F-92195 Meudon CEDEX, France

D. Mathiot
Centre National d'Etudes des Télécommunications de Grenoble, Centre Norbert Segard, Boîte Postale 98, 38243 Meylan CEDEX, France

(Received 6 May 1991)

Several deuteration experiments on crystalline silicon have been performed for various shallow dopant impurities (B and Al for *p*-type silicon; P and As for *n*-type silicon) and for different temperatures and times of plasma exposure. Deuterium diffusion depth profiles obtained by secondary-ion mass spectroscopy (SIMS) were simulated with an improved version of a previously reported model. A careful analysis of the SIMS data has allowed the reduction of the number of fit parameters, by excluding the H_2-molecule formation and by a rough estimate of the neutral-deuterium diffusion coefficient and of the surface concentration of neutral deuterium. The diffusion coefficients and related activation energies of the hydrogen species H^0, H^-, and H^+ were determined, leading to a stated ranking of the mobilities in the order $H^0 < H^- < H^+$. The dissociation energies of BH, AlH, and PH complexes were also calculated and have allowed us to deduce the corresponding bonding energies of the complexes, which suggest a scaling of the complex stability in the order PH < BH < AlH. Free-carrier depth profiles obtained by high-frequency capacitance-voltage measurements, combined with chemical etching, provided direct evidence of the rate of passivation of the shallow *p*-type-dopant impurities. The comparison between both couples of depth profiles (deuterium diffusion and carrier concentrations), in the case of *p*-type silicon, showed good agreement between the deactivation process of dopants and the corresponding depth penetration of deuterium.

I. INTRODUCTION

The fortuitous discovery of *p*-type-dopant deactivation by hydrogen incorporation in crystalline silicon[1] and subsequently in other widely used semiconductors has stimulated intense activity in this domain.[2,3] Because of its potential impact on semiconductor science and device technology,[4] much attention has been focused on the behavior of hydrogen in these materials and especially in crystalline silicon. Beside the diffusion processes and kinetic motion of hydrogen, the focus was mainly on its charge states and induced deep levels, possible bonding and complex formation with shallow dopants, microscopic configuration and passivating efficiency.[2,3] Debonding and recovery mechanisms were also investigated under peculiar conditions of annealing treatments, applied bias and temperature.[5-7] At present, it is well established that, in *p*-type silicon, H has a preferred positive charge state[5] with a deep donor level E_d near the midgap.[8] In addition, hydrogen pairing with a *p*-type dopant to form H-acceptor complexes is described[8] as a consequence of the electrostatic interaction between the positive H^+ ion and the negatively ionized acceptor A^-, both arising from a direct compensation process. Evidence for the *H*-acceptor complex configuration and its stability is well documented experimentally[9-11] and theoretically.[12-14] The most energetically favorable site of interstitial hydrogen is the bond center position, lying between the substitutional dopant and the host silicon atom and slightly off the $\langle 111 \rangle$ axis.[15]

For hydrogenated *n*-type silicon, earlier papers reported slightly passivating effects[16] and more evident hydrogen-donor complex formation.[17] Experimental results,[10,17] supported by theoretical calculations,[13,14,16-19] strongly suggest a trigonal symmetry for this complex, where the H atom is antibonded to one of the donor's neighbors. By analogy with the mechanisms described above for *p*-type, it was suggested that H^- could be the stable charge state of H in *n*-type Si, with a deep acceptor level in the gap.[20] Recently, two studies[21,22] have reported a set of capacitance-voltage measurement data of reverse-biased hydrogenated annealed *n*-type Si diodes, which were interpreted by the authors as the clearest evidence of the existence of H^- in the donor-doped silicon, although similar results have been explained by an alternative approach excluding the need for H^-.[23] Nevertheless it seems that the deactivation mechanism in *n*-type Si differs from that in *p*-type in many aspects such as a smaller deactivation efficiency and a less stable H-donor complex. The passivating effect in the *n*-type case could then be due only to the pairing occurrence.[8]

In order to investigate the behavior of hydrogen during deactivation, numerous studies and analyses have been proposed in the literature.[24-27] The large discrepancies observed in the extracted parameters such as diffusivities of hydrogen species, H-dopant bonding and debonding rates, activation and dissociation energies, are essentially due to the different physical assumptions assumed in the proposed models.

The above-mentioned observations[5,21,22] are consistent

 ©1991 The American Physical Society

with a recent model proposed by one of us,[28] where it was assumed that the behavior of hydrogen is governed by the three charge states H^0, H^+, and H^-. In addition, the possible formation of H_2 molecules was also considered. This model was subsequently used to simulate various deuterium profiles in *p*-type silicon[29] with the additional assumption of possible H_2 formation from H^0 and H^+ as suggested by some authors.[30] Although good fits were obtained for various doping levels, the authors have noticed the lack of good simulation of the shoulder or transition region in the diffusion profile of medium B-doped Si (10^{17} cm^{-3})—also observed in the literature for analogous profiles[31,32]—which appears between the near surface layer of defects and traps arising from plasma damage and the plateau at the doping level. Similarly, the deuterium profiles in *n*-type Si exhibit a region where the deuterium concentration exceeds the dopant concentration by at least one order of magnitude, as has also been reported previously.[15,20,21,32] Since this region in *n*-type Si is analogous to the shoulder observed in the *p* type, both could then be attributed to the diffusion of the same species which we suppose here to be neutral hydrogen. With an improved version of the previously reported model,[28] based on this physical assumption suggested by the experimental data, we propose a better simulation of the diffusion profiles in medium and highly *p*- and *n*-type doped Si at different deuteration temperatures and times of exposure. Capacitance-voltage measurements of deuterated *p*-type doped Si, combined with chemical etching, are also reported and discussed.

II. EXPERIMENT

p- and *n*-type floating-zone (FZ) crystalline silicon samples of different dopant concentrations were exposed to a radio-frequency (13.56 MHz) deuterium plasma of constant pressure (1 mbar) and power (0.12 W/cm^2), free of residual oxygen and water contamination. The deuteration was controlled with an accuracy of better than 1 °C and the samples were then rapidly cooled.

The depth deuterium profiles were obtained by secondary-ion mass spectroscopy (SIMS). The SIMS equipment was a Cameca IMS4f using a primary ion beam of cesium rastered over a large area in comparison with the analyzed one, in order to obtain a high depth resolution. The absolute concentrations were determined by calibration with respect to deuterium ion-implanted reference samples and the depth scales were established from measurements of the sputter-induced craters using a Talystep stylus profilometer (sensitivity ≈ 200 Å).

The active acceptor concentration profiles were obtained on *p*-type silicon from capacitance-voltage measurements using a conventional mercury diode (drop contact area$=2\times10^{-3}$ cm^2), connected to a digital Hewlett Packard LCR meter; the frequency of the ac signal was 1 MHz and the applied reverse voltage varied from 0 to -1 V. The *C*-*V* measurements with the Hg diode were combined with sequential chemical etching of silicon layers performed in an acidic solution 16HNO_3: 3CH_3CO_2H: 1HF. The etching rate, as evaluated by step height profilometry, was ≈ 2 μm/min. Some experiments, performed with a (*p*-type Si)/Al diode, have provided the same active acceptor concentrations profiles as that of the (p-type Si)/Hg diode.

III. RESULTS

We shall describe below first the experimental diffusion profiles of deuterium as provided by the SIMS measurements for *p*- and *n*-type silicon. Secondly, we shall comment on the experimental *C*-*V* profiles of free carriers as obtained by the (*p*-type silicon)/mercury Schottky diode.

A. Deuterium diffusion profiles in *p* type

Figure 1 shows a set of experimental diffusion profiles of deuterium in medium boron-doped silicon at 10^{17} and 2.5×10^{17} cm^{-3} for different deuteration times and temperatures. As already noticed, a transition region, or shoulder of excess deuterium concentration with respect to the doping level, is observed on each profile. It starts at the edge of the near surface layer of defects and traps resulting from plasma damage and ends by a plateau at the dopant concentration which is originated by the formation of neutral H-acceptor complexes. For a fixed temperature, the shoulder appears larger and more pronounced for the lower doping levels. For a given boron concentration, its width increases with either the deuteration time or temperature, or both. It may also be noticed that, once the contribution of the plateau at the dopant concentration level is subtracted from the shoulder, the resulting profile of the transition region follows a complementary error function, suggesting a diffusion of noninteractive species of one type, which we assume to be neutral deuterium.

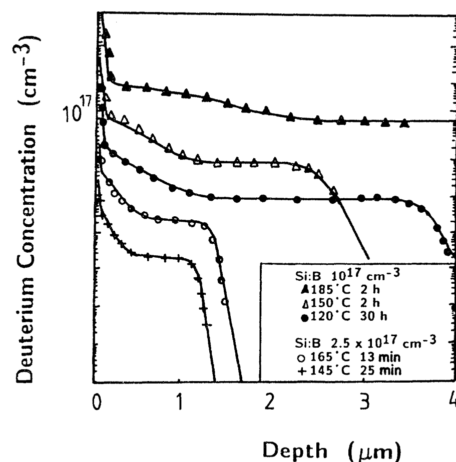

FIG. 1. SIMS depth profiles of deuterium diffusion in 10^{17} and 2.5×10^{17} boron-doped silicon. The solid line is the calculated profile. For the sake of clarity, the curves are shifted successively by one decade from the top. The 10^{17} cm^{-3} level on the figure is related to the upper curve. The fit parameters D_{H^0}, D_{H^+}, and k'_{BH} are reported in Table. I.

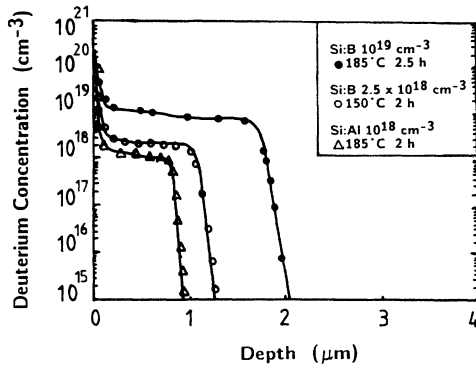

FIG. 2. SIMS depth profiles of deuterium diffusion in 2.5×10^{18}, 10^{19} cm^{-3} B-doped Si and in 10^{18} cm^{-3} Al-doped silicon. The solid line is the calculated profile. The fit parameters D_{H^0}, D_{H^+}, k'_{BH}, and k'_{AlH} are reported in Table I.

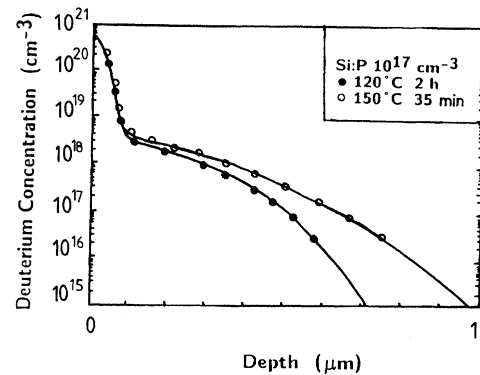

FIG. 4. Deuterium diffusion profiles in 10^{17} cm^{-3} P-doped Si. The solid line is the calculated profile. The fit parameters D_{H^0}, D_{H^-}, and k'_{PH} are reported in Table II.

Figure 2 shows another set of experimental diffusion profiles of deuterium in highly doped silicon: 2.5×10^{18} and 10^{19} cm^{-3} B dopant at 150 °C and 185 °C, respectively, and of 10^{18} cm^{-3} Al dopant at 185 °C. In all these profiles, we note the absence of the marked shoulder mentioned earlier, and for the Al profile, the smooth slope of the plateau and the abrupt subsequent decay. These observations seem consistent with the existence of a high proportion of neutral H-acceptor complexes which could be more stable for aluminum than boron.

B. Deuterium diffusion profiles in *n* type

The experimental diffusion profiles of deuterium, obtained after a deuteration at 120 °C and 150 °C of phosphorus-doped silicon at 10^{16} and 10^{17} cm^{-3} are shown, respectively, on Figs. 3 and 4. As already mentioned, one observes in these profiles an excess of deuterium concentration above the dopant level, starting at some 10^{18} cm^{-3}, and which appears more important for the lower doping (10^{16} cm^{-3}) profile than that of the higher doping one (10^{17} cm^{-3}). This excess is reminiscent of the shoulder reported in Fig. 1 for about 10^{17} cm^{-3} B-doped Si—similar slope and sharpness of a complementary error function—and may be attributed to the diffusion of the same noninteractive species of one type assumed to be neutral deuterium whose behavior does not differ from *p*- to *n*-type silicon.

Figure 5 shows two experimental diffusion profiles of deuterium in highly phosphorus (6×10^{18} cm^{-3}) and arsenic (6×10^{19} cm^{-3}) doped silicon. Although the excess of deuterium concentration above the dopant level is greatly decreased, the profiles do not exhibit any plateau at the doping level, as seen for *p*-type where it is usually attributed to the formation of neutral complexes.

C. *C-V* profiling of deuterated *p*-type Si

In order to determine the net carrier concentration $N(x)$ at a depth x, we have used the standard *C-V* profile

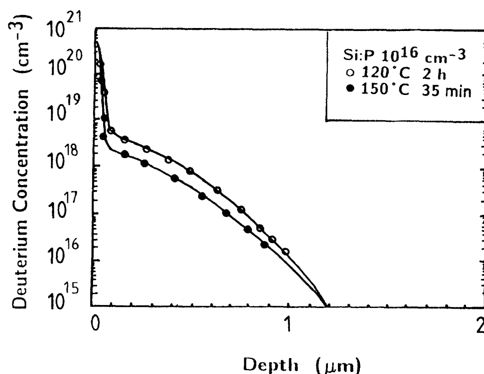

FIG. 3. Deuterium diffusion profiles in 10^{16} cm^{-3} P-doped Si. The solid line is the calculated profile. The fit parameters D_{H^0}, D_{H^-}, and k'_{PH} are reported in Table II.

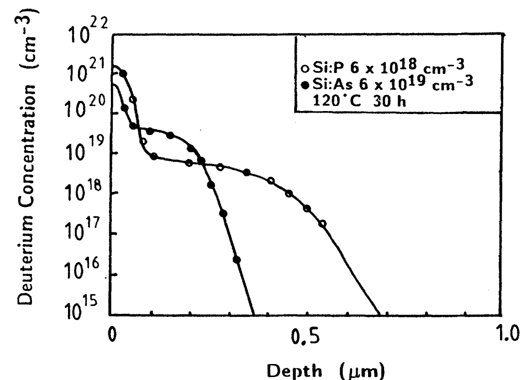

FIG. 5. SIMS depth profiles of deuterium in 6×10^{18} cm^{-3} P-doped silicon and in 6×10^{19} cm^{-3} As-doped Si. The solid line is the calculated profile. The fit parameters D_{H^0}, D_{H^-}, k'_{PH}, and k'_{AsH} are reported in Table II.

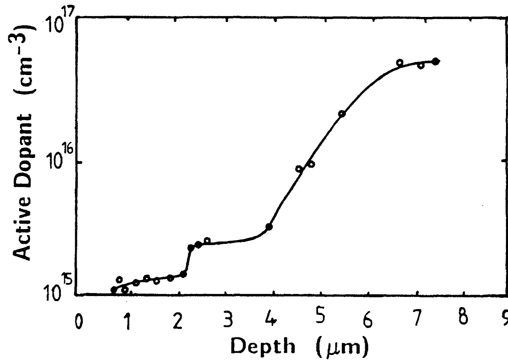

FIG. 6. Depth profile of active dopants by capacitance-voltage measurements of 10^{17} cm^{-3} B-doped Si deuterated at 120 °C for 30 h.

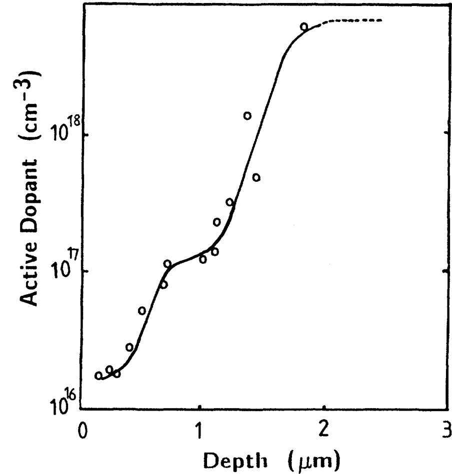

FIG. 8. Depth profile of active dopants by capacitance-voltage measurements of 10^{19} cm^{-3} B-doped Si deuterated at 185 °C for 2.5 h.

measurement combined with a layer-etching removal technique in the above-mentioned mixture of acids. As illustrated in Figs. 6–9, a series of sequential C-V measurements is performed after each etching of the sample. The measured carrier concentration $N(x)$ corresponds in fact to a depletion width x, and is given by

$$N(x) = -\frac{C^3}{\epsilon e S^2 \, dC/dV} , \tag{1}$$

with x expressed in terms of C, the capacitance of a voltage-dependent parallel-plate capacitor separated by the space-charge region, S the area of the drop mercury contact, and ϵ the dielectric constant of silicon:

$$x = \frac{\epsilon S}{C} . \tag{2}$$

Figures 6 and 7 illustrate the active carrier profiles in 10^{17} cm^{-3} B-doped silicon deuterated at 120 °C and 185 °C, respectively. Figures 8 and 9 show the corresponding profiles of higher dopant concentration of B (10^{19} cm^{-3}) and Al (10^{18} cm^{-3}), both exposed to a deuteration temperature of 185 °C. The overall shape of each active carrier profile reflects that of the corresponding one of deuterium diffusion as revealed by SIMS measurements. It is worth noting that, in contrast with the Al-doped profile, all the B-doped ones exhibit a somewhat small abrupt enhancement of the active carrier at about 2 μm depth for the 10^{17} cm^{-3} concentration and near 0.5 μm for the 10^{19} cm^{-3} one, i.e., largely beyond the plasma damaged layer. Although the deactivation effect of deuterium is better than 98% in all cases, regardless of the dopant type and deuteration temperature, the above-mentioned small enhancement for the B dopant profile seems significant, especially for the medium concentration (10^{17} cm^{-3}), if we take into account the statistical distribution of the experimental points. As for the overall shape of the C-V profiles, we notice the smoothness of the increasing of the active acceptor for high-temperature deuteration (185 °C) in medium doped silicon which contrasts

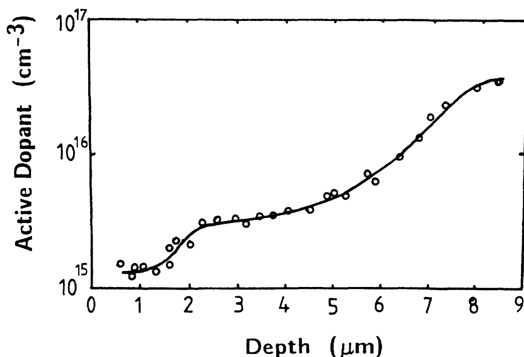

FIG. 7. Depth profile of active dopants by capacitance-voltage measurements of 10^{17} cm^{-3} B-doped Si deuterated at 185 °C for 2 h.

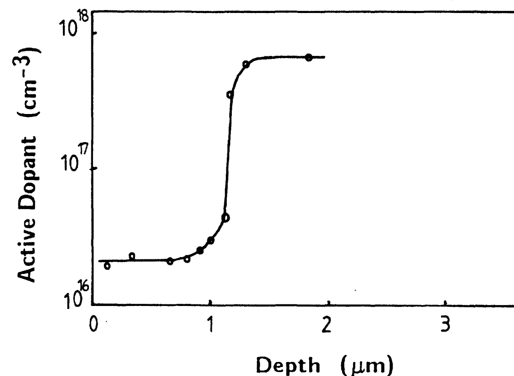

FIG. 9. Depth profile of active dopants by capacitance-voltage measurements of 10^{18} cm^{-3} Al-doped Si deuterated at 185 °C for 2 h.

with the sharpness of the corresponding variation in Al-doped silicon, although the latter is deuterated at the same temperature and with the same time of exposure.

IV. MODELING OF DEUTERIUM DIFFUSION

Apart from the characteristic plateau at the doping level for p-type, the main common feature of the reported experimental profiles is the appearance of a shoulder in the medium doped p-type profile and the existence of an excess deuterium concentration in that of n type: both are found to be similar in shape and follow a complementary error function which could be due to the diffusion of noninteractive species of one type. In this context, we have assumed that these diffusing species are neutral deuterium in both cases: the shoulder in p type and the excess in n type. This assumption can be supported by the following argument as illustrated by the energy diagrams sketched in Figs. 10 and 11 for p- and n-type silicon, respectively.

Let l and W_i be, respectively, in Fig. 10, the depth of the damaged surface layer and the width of the band bending between the surface and the bulk. When the initial concentration of dopant is increased, W_i decreases ($W_1 > W_2 > W_3$) as expected, but l could be assumed to remain nearly constant. Since it is generally accepted[8,24,28] that the deep donor level E_d of H in p-type Si lies somewhere near the midgap, the crossing between E_d and the Fermi energy level E_F will occur at a depth L_i from the surface which is narrowed by a raising of the dopant concentration ($L_1 > L_2 > L_3$). For the medium doping case [Fig. 10(a)], $L_1 \gg l$, the relative concentration of neutral hydrogen $[H^0]/[H^+]$ is important and we observe then a complementary error type function diffusion profile. For a higher doping level, the band bending becomes important [Fig. 10(b)], E_F moves towards the valence band, and the depths L_2 and l are then comparable ($L_2 \geq l$), leading to a decrease of $[H^0]/[H^+]$ and then to a less pronounced shoulder. As for the limit case of high concentration [Fig. 10(c)], probably greater than 10^{18} cm^{-3}, E_F approaches more closely the valence band, the cross depth L_3 could be small enough to be contained in the surface defect layer ($L_3 \leq l$), and the above-mentioned shoulder would not be observed (Fig. 2). This may be compared with the case of deuterated Zn-doped GaAs,[33] where a similar shoulder is observed for concentrations up to 10^{19} cm^{-3}; in that case, the shoulder is assigned to the diffusion of neutral deuterium and the best fits are obtained for a deep donor level of H, located at 1.1 eV from the conduction band, i.e., in the lower half of the band gap. Therefore, in the light of our energy diagram of Fig. 10, the limit case in Zn-doped GaAs would correspond to a concentration of the order of 10^{19} cm^{-3}.

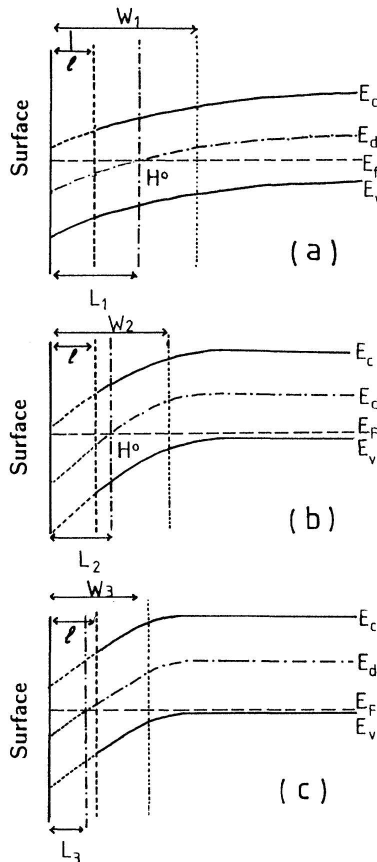

FIG. 10. Energy diagram of band bending for p-type silicon (see text). l is the thickness of the plasma-damaged layer; W_i, the depth of the depletion region; E_c and E_v, the edges of the conduction and valence bands, respectively; E_F, the Fermi level; E_d, the deep donor level of H.

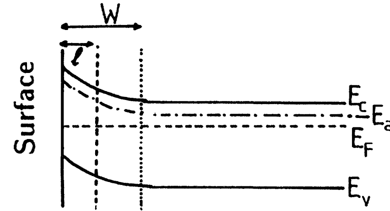

FIG. 11. Energy diagram of band bending for n-type silicon (see text). E_a is the acceptor level of H; the other parameters are the same as in Fig. 10.

Concerning the n-type Si case, the same approach of explanation may be attempted with the appropriate energy diagram as plotted in Fig. 11 where we adopt the same above-mentioned parameters. However, owing to the less effective passivation effect observed in the n-type-doped material, it is reasonable to assume that the deep acceptor level E_a assigned to hydrogen could in this case be in the upper half of the band gap, even above the Fermi level E_F. So, in the depletion layer, where the spacing between E_a and E_F is more important than in the bulk, the relative concentration of $[H^0]$ with respect to $[H^-]$ would be high, leading to the large excess of deuterium concentration which we observe (Figs. 3 and 4). Therefore,

when the n dopant concentration is increased, E_F moves toward the conduction band and the spacing between E_a and E_F becomes less important, leading to a decrease of the ratio $[H^0]/[H^-]$ which is consistent with a vanishing of the excess of deuterium as observed in the high doped material (Fig. 5).

These observations and assumptions lead us to rule out the possible formation of hydrogen molecules as suggested by the diffusion model reported previously.[28,29] We consider here that in p- (n-) type Si, hydrogen can exist in the two charge states H^0 and H^+ (H^-) and the only permitted reaction is between H^+ (H^-) and the ionized A^- (D^+) acceptor (donor) dopant to form neutral complexes.

$$H^+ + A^- \underset{k'_{AH}}{\overset{k_{AH}}{\rightleftharpoons}} (AH)^0 \tag{3a}$$

or respectively,

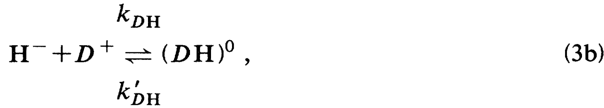

$$H^- + D^+ \underset{k'_{DH}}{\overset{k_{DH}}{\rightleftharpoons}} (DH)^0 \,, \tag{3b}$$

where k'_{AH} (or k'_{DH}) is the dissociation frequency of the complex and the rate coefficient k_{AH} (or k_{DH}) is expressed in terms of the diffusivity D_{H^+} (D_{H^-}) of H^+ (H^-) and the Coulombic capture radius $r_c = e^2/\epsilon kT$. The relative concentrations of H^0 and H^+ (H^-) depend on the local Fermi-level position as follows:

$$\frac{[H^+]}{[H^0]} = \exp[(E_d - E_F)/kT] \tag{4a}$$

or

$$\frac{[H^-]}{[H^0]} = \exp[(E_F - E_a)/kT] \,, \tag{4b}$$

respectively.

As H^0 and H^+ (H^-) are assumed to be mobile, the total flux of H is due to the individual contributions of H^0 and H^+ (H^-) given by the first Ficks law:

$$J_{H^0} = -D_{H^0} \frac{\partial [H^0]}{\partial x} \,, \tag{5}$$

$$J_{H^+} = -D_{H^+} \frac{\partial [H^+]}{\partial x} - D_{H^+}[H^+] \frac{1}{n}\frac{\partial n}{\partial x} \,, \tag{6a}$$

or respectively,

$$J_{H^-} = -D_{H^-} \frac{\partial [H^-]}{\partial x} + D_{H^-}[H^-] \frac{1}{n}\frac{\partial n}{\partial x} \,. \tag{6b}$$

The last term in J_{H^+} (J_{H^-}) is due to the built-in electric field, and the local density of free carriers, n, is obtained by solving Poisson's equation.

The evolution of the various concentrations can then be calculated by the following system of equations:

$$\frac{\partial [H]^{tot}}{\partial t} = -\frac{\partial [J_{H^0} + J_{H^+}]}{\partial x} \,, \tag{7}$$

$$\frac{\partial [AH]}{\partial t} = k_{AH}[A^-][H^+] - k'_{AH}[AH] \,, \tag{8}$$

for p type, or respectively,

$$\frac{\partial [H]^{tot}}{\partial t} = -\frac{\partial [J_{H^0} + J_{H^-}]}{\partial x} \,, \tag{9}$$

$$\frac{\partial [DH]}{\partial t} = k_{DH}[D^+][H^-] - k'_{DH}[DH] \,, \tag{10}$$

for n type. $[H]^{tot}$ is the total concentration of hydrogen including $[H^0]$, $[H^+]$ (or $[H^-]$), $[AH]$ (or $[DH]$) and other trapped hydrogen $[T_rH]$ on surface defects due to plasma damage. Indeed, such $[T_rH]$ extra trapping is necessary to accurately simulate the surface region of the hydrogen profiles. It is described by an empirical distribution of traps[28] following a Gaussian shape:

$$[T]^{tot} = [T]_0 \exp(-x^2/L^2) \,. \tag{11}$$

V. BEST FITS

A. p type

Beside the exclusion of H_2-molecule formation, we adopt for neutral deuterium a diffusion coefficient as deduced from an estimate of the net penetration depth of the shoulder observed in medium doped silicon from which we start our fit procedure. In addition to this approach of reduced fitting parameters, the calculated profiles for a dopant concentration near 10^{17} cm^{-3} depend strongly on the position of the deep donor level E_d (i.e., the ratio $[H^+]/[H^0]$) and permit an accurate determination of the thermodynamic parameters governing the hydrogen behavior in silicon. Among these profiles, we have chosen to begin with that corresponding to the lowest deuteration temperature (120 °C) and higher time of exposure (30 h) because of its sensitivity to the dissociation frequency k'_{AH} which determines the slope of the sharp hydrogen profile.

The best fits are obtained for E_d at 0.52 eV from the conduction band which is the same as the reported value in a previous paper.[28] The calculated and experimental diffusion profiles are compared in Fig. 1 for about 10^{17} cm^{-3} B-doped silicon and in Fig. 2 for boron and aluminum dopant concentrations beyond 10^{18} cm^{-3}. All the simulated profiles for B and Al and for all deuteration temperatures and times of plasma exposure are obtained for the same above-mentioned value of E_d. The remaining fitting parameters used for these simulations are reported in Table I. We find that these parameters, in addition to the unique value of E_d, enable us to obtain in all cases a good description of the experimental profiles and especially those of the transition region which we attribute to neutral deuteration diffusion.

B. n type

As a consequence of the assumption of a neutral deuterium diffusion expected to be responsible for the excess of deuterium concentration above the dopant level, according to its similarity with the shoulder in the medium doped p-type profiles and the above detailed arguments, we adopt in the present simulations the same diffusion values of neutral deuterium D_{H^0} as reported for p-type Si

TABLE I. Fitting parameters for deuterium diffusion in p-type silicon. D_{H^0} is the neutral deuterium diffusion coefficient, D_{H^+} is the positively charged deuterium diffusion coefficient, and k'_{AH} is the dissociation frequency of the deuterium-acceptor complex.

Doped samples	T (°C)	Time	D_{H^0} ($cm^2 s^{-1}$)	D_{H^+} ($cm^2 s^{-1}$)	k'_{AH} (s^{-1})
Si:B(10^{17} cm^{-3})	185	2 h	5×10^{-12}	3×10^{-11}	7×10^{-1}
Si:B(10^{17} cm^{-3})	150	2 h	3.6×10^{-13}	8×10^{-12}	8×10^{-2}
Si:B(10^{17} cm^{-3})	120	30 h	4×10^{-14}	2.5×10^{-12}	5×10^{-3}
Si:B(2.5×10^{17} cm^{-3})	165	13 min	7.5×10^{-13}	1.3×10^{-11}	2×10^{-1}
Si:B(2.5×10^{17} cm^{-3})	145	25 min	2.5×10^{-13}	6×10^{-13}	5×10^{-2}
Si:B(10^{19} cm^{-3})	185	2.5 h	3.6×10^{-12}	1×10^{-12}	8.5×10^{-1}
Si:B(2.5×10^{18} cm^{-3})	150	2 h	3.5×10^{-13}	5.5×10^{-13}	7.5×10^{-2}
Si:Al(10^{18} cm^{-3})	185	2 h	4.0×10^{-12}	1.3×10^{-14}	10^{-2}

in Table I. With a surface concentration of neutral deuterium H_S of some 10^{18} cm^{-3} as extrapolated from the onset of the deuterium profile in the bulk, this assumption leads to an additional reduction of the fit parameters of the model.

We start our fit procedure on the profiles of 10^{16} cm^{-3} phosphorus-doped silicon where the shape of deuterium profiles, dominated by an excess of about two orders of magnitude of deuterium concentration above the dopant level, reveals a great sensitivity to the deep acceptor level E_a of hydrogen and then to the relative concentration of $[H^-]$ and $[H^0]$, i.e., to the ratio $[H^-]/[H^0]$ according to Eq. (4b).

However, the simulation of the 10^{16} cm^{-3} profiles exhibits much less sensitivity to the diffusion coefficient of H^-, D_{H^-}, and the dissociation frequency k'_{DH}. This situation appears reasonable on the basis of the small relative concentration of H^-, $[H^-]$, with respect to that of H^0, $[H^0]$, according to Eq. (4b). This arises from the important spacing between E_a and E_F as illustrated in Fig. 11. Therefore the calculated profile in the 10^{16} cm^{-3} case allows the determination of a rather precise value of E_a at 0.06 eV from the conduction band, which is the same as the reported value in a previous paper,[28] and rough values of D_{H^-} and k'_{DH}. These last parameters are subsequently established with much more refinement by the simulation of the 10^{17} cm^{-3} profiles.

In Fig. 5, we compare the simulated and experimental profiles of diffusing deuterium in highly doped n-type silicon at about 6×10^{18} phosphorus and 6×10^{19} arsenic cm^{-3} concentrations, respectively, as obtained for the same value of the deep acceptor level, E_a, of hydrogen, i.e., at 0.06 eV from the conduction band.

All the fitting parameters used in the reproduction of the SIMS profiles in n-type silicon are reported in Table II, and have yielded, in all cases, a good simulation of the experimental diffusing profiles of deuterium.

VI. DISCUSSION

We have attempted in our study to take into account the possible effects and interactions, and have reduced the number of fitting parameters by a careful observation of the data. In this respect, we have discussed the exclusion of hydrogen-molecule formation and, from the experimental data, we have suggested a rough estimate of both the neutral deuterium diffusion coefficient and the initial surface concentration of deuterium. As we proceeded to the simulation of a large number of experimental profiles, the remaining fitting parameters, such as the deep level of hydrogen E_d or E_a, the diffusion coefficient of H^+ or H^-, and the dissociation frequency k'_{AH} or k'_{DH} could then be deduced with a good precision.

We shall discuss first the deduced values of deep levels of hydrogen. All the simulations of the deuterium diffusion profiles in the p-type samples were obtained

TABLE II. Fitting parameters for deuterium diffusion in n-type silicon; D_{H^0}, the H^0 diffusion coefficient; D_{H^+}, the diffusion coefficient of H^+; k'_{DH}, the dissociation frequency of the deuterium-donor complex.

Doped samples	T (°C)	Time	D_{H^0} ($cm^2 s^{-1}$)	D_{H^-} ($cm^2 s^{-1}$)	k'_{DH} (s^{-1})
Si:P(10^{16} cm^{-3})	120	2 h	4×10^{-14}	7.5×10^{-13}	3.2×10^{-3}
Si:P(10^{16} cm^{-3})	150	35 min	3.6×10^{-13}	4×10^{-12}	4×10^{-2}
Si:P(10^{17} cm^{-3})	120	2 h	4×10^{-14}	7.5×10^{-13}	3.2×10^{-3}
Si:P(10^{17} cm^{-3})	150	35 min	3.6×10^{-13}	4×10^{-12}	4×10^{-2}
Si:P(6×10^{18} cm^{-3})	120	30 h	4×10^{-14}	1×10^{-13}	3.2×10^{-2}
Si:As(6×10^{19} cm^{-3})	120	30 h	4×10^{-14}	5×10^{-15}	1.5×10^{-2}

with a deep donor level E_d at 0.52 eV from the conduction band. This value leads to a location of E_d near the midgap, in agreement with other predicted or deduced values in the literature.[8,24,28] Furthermore, such location of E_d, slightly above the midgap, reflects a high relative concentration of H^+ with respect to H^0, supporting a passivation mechanism due to compensation, as proposed by Pantelides.[8] This situation explains then the high rates of passivation observed in hydrogenated *p*-type silicon[34] and confirmed in our capacitance-voltage measurements (Figs. 6–9).

For *n*-type silicon, the best simulations were obtained with a deep acceptor level E_a at only 0.06 eV from the conduction band. This value, determined by the first approach of fitting in the lower concentration (10^{16} cm^{-3}) case, where other parameters exhibit much less influence, seems reasonable on the basis of some important observations and major arguments. Indeed, as we observe in all the depth profiles an excess of deuterium concentration which decreases when the Fermi level E_F moves towards the conduction band due to increasing the dopant concentration, E_a must be located above E_F. This conclusion results from the assignment of this excess of deuterium to neutral species which leads to a less visible plateau at the doping level. Moreover, the low rate of the passivation effect reported in medium doped *n*-type silicon,[21,22] compared with that observed in our *C-V* profiles data (Figs. 6–9) and related results[34] for *p* type, may arise also from an acceptor level of H in the *n*-type materials lying between E_c and E_F. As a final comment, we observe that an E_a level at 0.06 eV recalls one of the two deep levels observed by Johnson *et al.*[32] in hydrogenated *n*-type silicon. According to the authors, these deep levels are generated by the diffusing hydrogen in the subsurface zone of low phosphorus-doped silicon and may arise from a weak bond of interstitial hydrogen with Si or an unidentified impurity. Since the configuration of interstitial hydrogen at the antibonding site of a silicon nearest neighbor of substitutional *n*-type dopant is the most generally accepted stable position,[14,16–19,35] this configuration could be presumably at the origin of both a likely attribution of E_a to H—Si. . .P antibonding and the moderate degree of passivation due to hydrogen in *n*-type silicon.[21,22]

Concerning the neutral deuterium diffusion coefficient, it is worth noting that all the simulations in *p*- and *n*-type materials are obtained with D_{H^0} dependent only on the temperature. The D_{H^0} of Tables I and II are reported in Fig. 12. From the Arrhenius plot of $D_{H^0}(T) = D_0 \exp(-E_{act}/kT)$, we deduce an activation energy E_{act} of about 1.12 eV and a preexponential factor D_0 of about 8.4 $cm^2\,s^{-1}$. While these values of D_{H^0} agree with some of the corresponding ones reported in the literature,[36–38] they are one order of magnitude greater than those obtained by Capizzi and Mittiga,[24] and several orders of magnitude lower than those adopted by other authors[27,28] as extrapolated from the pioneering work of Van Wieringen and Warmoltz (VW).[39] In this context, we mention that good reproductions of experimental data could be obtained with appropriate couples of values of

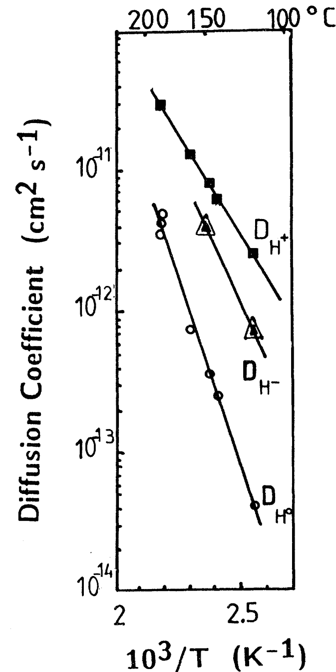

FIG. 12. Arrhenius plots of D_{H^0} for all samples, D_{H^+} for *p*-type silicon doped to concentrations of 10^{17} and 2.5×10^{17} B cm^{-3}, and D_{H^-} for *n*-type silicon doped to 10^{16} and 10^{17} P cm^{-3}.

D_{H^0} and H_S, the surface concentration of neutral hydrogen, in which cases the product $H_S D_H$ seems constant.[40] A relatively low H_S leads to a high D_{H^0} and vice versa. Indeed, when H_S is taken at about 10^{14} cm^{-3}, the reported values of D_{H^0} (Refs. 27 and 28) are close to those of VW, but lead to a lower diffusion coefficient of H^+, D_{H^+}, when one attempts to fit the experimental deuterium diffusion profiles in *p*-type doped silicon.[28,29] However, this set of H_S, D_{H^0}, and D_{H^+} values does not allow a good description of the above-mentioned shoulder in the medium concentration B-doped silicon. Since in this latter case the data suggest an H_S of some 10^{18} cm^{-3}, the shoulder is best fitted with this value of H_S and a D_{H^0} value several orders of magnitude lower than that of VW.

In order to explain the discrepancies observed between numerous deduced D_{H^0} values and that extrapolated from the VW work, it has been speculated that the diffusing species in the VW study could be H^+ whose diffusion coefficient is expected to be larger than that of H^0. However, it is not clear to us whether or not the VW data correspond to H^+ diffusion. Indeed, as it is now widely accepted and confirmed by this work, E_d must be near the midgap in the current deuteration temperature, i.e., at about 0.5 eV below E_c. Then if we assume as usual that this donor level remains fixed to E_c, the dominant charge state is H^0 near 1000 °C in the VW study, where the intrinsic Fermi level is about 0.4 eV below E_c, i.e.,

significantly above E_d. As a matter of fact, as depicted in Fig. 13, our deduced D_{H^0} values extrapolate correctly to the VW high-temperature data. The resulting best correlated Arrhenius plot of Fig. 13 allows us to extract an activation energy E_{act} of about 1.03 eV and a preexponential factor D_0 near 0.6 $cm^2 s^{-1}$. The latter deduced value of E_{ac} is still close to the former one (1.12 eV), and one could then estimate that this approach would bring an insight into the solution to the existing discrepancy between the "reduced" diffusivity of H obtained at moderate temperatures[36–38] and the extrapolated one from the high-temperature data of VW.[39] It could shed some light on the other mentioned explanation based on the possible trapping and detrapping of diffusing H^0 via the formation and dissociation of molecular and defect-molecular complexes.[41]

The preceding discussion may give rise to a question concerning the behavior of H^0 during cooling. Since from our operating temperature, a possible effusion of H during cooling can be safely excluded,[42] one has to consider some trapping processes and quenching mechanisms of this species. While the trapping of H on already formed H-dopant complexes has been suggested,[43] other competing configurations such as molecular hydrogen H_2 and metastable diatomic hydrogen complex H_2^* were also reported by theoretical studies.[44,45] However, in addition to the exclusion of H_2 formation in the present study, other quantitative descriptions have not successfully reproduced the data when molecular formation was taken into account.[24,29] Furthermore, because of the large binding energy and the high diffusion barrier of molecular hydrogen (2–3 eV),[2,46] a H_2 diffusion mode cannot explain the diffusivity data. Therefore, from our point of view, the energetically favorable configuration of a H_2^* complex[44,45] or some other defect-hydrogen complex, probably involving a dopant missed by the Pantelides passivation mechanism,[8] could occur during cooling. Since in the region of high concentration of H^0, the probability of formation of such configurations is increased, it is tempting to attribute to some "deactivating" defect hydrogen complex the slight additional passivation observed on *C-V* active dopant profiles in the region of high H^0 density, i.e., up to ≈ 2 μm in deuterated 10^{17} cm^{-3} B-doped silicon (Figs. 6 and 7). Such a slight increase is not clearly exhibited in the corresponding profile for Al (Fig. 9), and does not exceed 1% in the ≈ 0.5 μm depth of the deuterated 10^{19} cm^{-3} B-doped sample (Fig. 8). This could be a further indication of the smaller density of H^0 in these highly doped materials, as discussed earlier, in comparison with those of the medium doped ones.

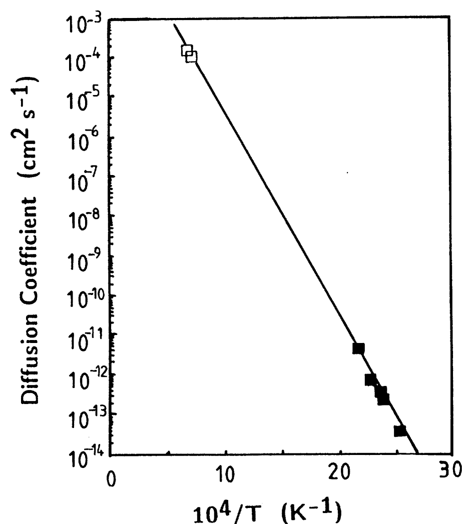

FIG. 13. Arrhenius plot of D_{H^0} including fit parameter values (closed squares) and VW values (Ref. 39) (open squares).

In contrast to D_{H^0}, the diffusion coefficient of H^+, D_{H^+}, appears to clearly depend on the concentration and nature of the dopant. When the dopant level is increased, $D_{H^+}(T)$ of a given temperature decreases as reported also in several studies.[27,29,47,48] Concerning the dopant type, we have obtained a relatively low value of D_{H^+} (1.3×10^{-14} $cm^2 s^{-1}$) for Al-doped silicon (10^{18} cm^{-3}) with respect to the corresponding one for B-doped silicon (5.5×10^{-13} $cm^{-2} s^{-1}$) in spite of the higher concentration (2.5×10^{18} cm^{-3}). This difference could be related to the larger dissociation energy of the AlH complex, estimated below at about 1.4 eV, compared with that of the BH complex evaluated hereafter at 1.19 eV. Analogous results were also obtained for *n*-type silicon where D_{H^-} varies inversely to the dopant concentration and is also dependent on the dopant type.

These observations may be interpreted by considering a similar influence of a high dopant concentration and a large dissociation energy on the diffusion path of either H^+ or H^-. This latter parameter may be then affected by both the decrease of the distance between two dopant traps which becomes comparable with the capture radius of the dopant when its concentration is enhanced, and an increase of the activation energy. In this context, the influence of doping on the diffusivity of hydrogen species in high B-doped silicon (i.e., of H^+) was analyzed in terms of an effective diffusion coefficient due to possible detrapping and retrapping events during the migration of hydrogen atoms.[47,48]

Nevertheless, for *p*-type and for medium B-doped silicon, i.e., at 10^{17} and 2.5×10^{17} cm^{-3}, the fit parameters values of D_{H^+} lie on a straight line in the Arrhenius plot of $D_{H^+}(T)=D_0^+\exp(-E_{act}^+/kT)$ in Fig. 12. They are, in the 120–185 °C temperature range, larger than the corresponding D_{H^0} values at the same temperature. One may explain this behavior as due to the higher mobility of H^+ between dopant traps in the lattice. Indeed, the deduced activation energy of D_{H^+} of about 0.60 eV is lower than that of D_{H^0} (1.03–1.12 eV). From the above equation, we derive a preexponential factor D_0^+ of the order of 1.2×10^{-4} $cm^2 s^{-1}$.

Concerning the diffusion coefficient of H^-, in contrast to its behavior in highly doped material as reported and explained above, we observe that the fit values for 10^{16}

and 10^{17} cm^{-3} phosphorus-doped silicon for each temperature agree well with the Arrhenius plot of Fig. 12. These values lie, in our operating temperature range, between those of D_{H^0} and D_{H^-}, and in the range suggested by Zhu, Johnson, and Herring.[22]

From $D_{H^-}(T)=D_0^- \exp(-E_{act}^-/kT)$ of Fig. 12, we can deduce an activation energy of H^-, E_{act}^-, of about 0.80 eV and a preexponential factor D_0^- of about 1.3×10^{-2} cm^2 s^{-1}. While E_{act}^- ranges between those of H^0 and H^+, 1.03–1.12 and 0.60 eV, respectively, as deduced above, it seems possible then to proceed, at least in the present deuteration temperature range, to a significant scaling of the corresponding mobilities in the order $H^0 < H^- < H^+$.

The last fit parameters values of the dissociation frequency k'_{AH} or k'_{DH} allow a good estimate of the dissociation energy of the appropriate complex. For *p*-type silicon, the k'_{BH} values of B-doped material were found to fit very well the straight line of the Arrhenius plot $k'_{BH}=\nu_{BH}\exp(-E_{BH}/kT)$ of Fig. 14 for all deuterium profiles regardless of the boron concentration. The calculated attempt frequency $\nu_{BH}\approx10^{13}$ s^{-1} seems reasonable and the deduced dissociation energy E_{BH} of 1.19 eV is in good agreement with those reported by the different works of Capizzi and Mittiga,[24] Mathiot *et al.*,[29] Zundel and Weber,[6] and also with the theoretical value (1.1 eV) calculated by Denteneer *et al.*[49] It is also possible to deduce from our calculated energies of BH complex dissociation and of H^+ migration the binding energy of the complex. From the reaction $(BH)^0 \rightleftharpoons B^- + H^+$, one can evaluate the binding energy as $1.19-0.60=0.59$ eV, in good agreement with that calculated (0.59 eV) theoretically[50] and that deduced in the experimental work (0.60 eV) of Herrero *et al.*[47]

Although we have only one experimental profile for 10^{18} cm^{-3} Al-doped silicon, we are tempted to proceed to an estimate of the dissociation energy of the AlH complex. By an analogous approach and an assumed atomic frequency ν_{AlH} of about 10^{13} s^{-1}, the fit parameter value k'_{AlH} of 10^{-2} s^{-1} leads to a dissociation energy E_{AlH} of about 1.36 eV. This value is close to that deduced by Zundel and Weber,[6] although they obtained 1.44 eV for $\nu_{AlH}\approx3.1\times10^{13}$ s^{-1} which corresponds to a value of 1.40 eV in our work. In all cases, E_{AlH} seems significantly higher than E_{BH} and suggests a more stable AlH complex than BH, consistent with the nearly horizontal plateau and the abrupt decay (respectively abrupt increase) of the Al-doped diffusion depth profile (respectively *C-V* depth profile).

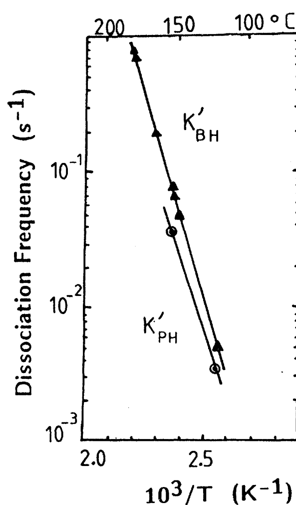

FIG. 14. Arrhenius plots of dissociation frequencies k'_{BH} and k'_{PH} for B-doped and P-doped (to 10^{16} and 10^{17} cm^{-3}) Si, respectively.

For *n*-type silicon, however, the dissociation frequency k'_{DH} seems dependent on the dopant concentration since it increases with the phosphorous level. A reasonable explanation could be based on the fact that a decrease in the mean distance between dopant traps could affect the stability of the complex in addition to the diffusion path of H^-. Nevertheless, the k'_{PH} values for 10^{16} and 10^{17} cm^{-3} were found to fit well the Arrhenius plot $k'_{PH}=\nu_{PH}\exp(-E_{PH}/kT)$ of Fig. 14. In an analogous approach to that of *p* type, we deduce a reasonable value of the attempt frequency $\nu_{PH}\approx10^{13}$ s^{-1} and a dissociation energy E_{PH} of about 1.21 eV. This latter value is in good agreement with that reported by Zhu, Johnson, and Herring,[22] and lies between those deduced by Bergman *et al.*[17] and Endrös, Krühler, and Grobmaier.[51] Finally, we have attempted to deduce from the calculated E_{PH} and E_{ac}^- values an estimate of the binding energy of the PH complex. The estimated value of the PH binding energy of about 0.40 eV lies in the range proposed by Zhu, Johnson, and Herring[22] and is significantly lower than the corresponding one for boron-doped silicon (0.59 eV), suggesting a rather less stable complex.

VII. SUMMARY

Good simulations of deuterium diffusion profiles in *p*- and *n*-type doped crystalline silicon have been performed with an approach excluding the hydrogen-molecule formation. The extracted best-fit parameters have allowed the following conclusions.

(i) A deep donor level for hydrogen exists near the midgap at 0.52 eV from the conduction band for *p*-type silicon and an acceptor level for hydrogen in the gap at only 0.06 eV from the conduction band exists for *n*-type silicon. Both are consistent with the related rates of passivation in the corresponding materials. While the deactivation in *p*-type Si could be due to the compensation mechanism, it could result, in the *n*-type material, from the pairing between H and the *n*-type dopant.

(ii) A good correlation is found between the extracted values of the diffusion coefficient of H^0 in the range 120–185 °C and those measured at high temperatures by VW. This approach has allowed us to deduce an activation energy which agrees well with those reported in the literature.

(iii) The observed scaling of the diffusivities of H^0, H^-, and H^+, in the operating temperature range, leads to a stated ranking of the corresponding mobilities in the order $H^0 < H^- < H^+$.

(iv) The calculated dissociation and binding energies of BH, AlH, and PH complexes provide a significant estimate of the relative stability of these complexes. While the binding energy of PH is lower than those of BH and AlH suggesting a less stable complex configuration in *n*-type than that in *p*-type material, it seems from the comparison between the dissociation energies that in the *p* type, the AlH complex is rather more stable than BH.

[1]C. Sah, J. Y. Sun, and J. J. Tzou, Appl. Phys. Lett. **43**, 204 (1983); **43**, 962 (1983).

[2]S. J. Pearton, J. W. Corbett, and T. S. Shi, Appl. Phys. A **43**, 153 (1987).

[3]J. Chevallier and M. Aucouturier, Annu. Rev. Mater. Sci. **18**, 219 (1988).

[4]S. J. Pearton, Defect and Diffusion Forum **62-63**, 1 (1989).

[5]A. J. Tavendale, D. Alexiev, and A. A. Williams, Appl. Phys. Lett. **47**, 316 (1985).

[6]T. Zundel and J. Weber, Phys. Rev. B **39**, 13 549 (1989); in *Impurities, Defects and Diffusion in Semiconductors: Bulk and Layered Structures,* edited by J. Bernhole, E. E. Haller, and D. J. Wolford, MRS Symposia Proceedings No. 163 (Materials Research Society, Pittsburgh, 1990), p. 443.

[7]C. H. Seager and R. A. Anderson, in *Impurities, Defects and Diffusion in Semiconductors: Bulk and Layered Structures* (Ref. 6), p. 431.

[8]S. T. Pantelides, Appl. Phys. Lett. **50**, 995 (1987).

[9]M. Stavola, S. J. Pearton, J. Lopata, and W. C. Dautremont-Smith, Appl. Phys. Lett. **50**, 1086 (1987); Phys. Rev. B **37**, 8313 (1988).

[10]K. Bergman, M. Stavola, S. J. Pearton, and T. Hayes, Phys. Rev. B **38**, 9643 (1988).

[11]B. Pajot, A. Chari, M. Aucouturier, M. Astier, and A. Chantre, Solid State Commun. **67**, 855 (1988).

[12]G. G. DeLeo and W. B. Fowler, Phys. Rev. B **31**, 6861 (1985); J. Electron. Mater. **14a**, 745 (1985); Phys. Rev. Lett. **56**, 402 (1986).

[13]K. J. Chang and D. J. Chadi, Phys. Rev. Lett. **60**, 1422 (1988).

[14]S. K. Estreicher, L. Throckmorton, and D. Marynick, Phys. Rev. B **39**, 13 241 (1989).

[15]A. D. Marwick, G. S. Oehrlein, and N. M. Johnson, Phys. Rev. B **36**, 4539 (1987).

[16]N. M. Johnson, C. Herring, and D. J. Chadi, Phys. Rev. Lett. **56**, 769 (1986).

[17]K. Bergman, M. Stavola, S. J. Pearton, and J. Lopata, Phys. Rev. B **37**, 2770 (1988).

[18]S. B. Zhang and D. J. Chadi, Phys. Rev. B **41**, 3882 (1990).

[19]P. J. H. Denteneer, C. G. Van de Walle, and S. T. Pantelides, Phys. Rev. B **41**, 3885 (1990).

[20]N. M. Johnson and C. Herring, Phys. Rev. B **38**, 1581 (1988); Proceedings of the 15th International Conference on Defects in Semiconductors, edited by G. Ferenczi [Mater. Sci. Forum **38-41**, 961 (1989)].

[21]A. J. Tavendale, S. J. Pearton, and A. A. Williams, Appl. Phys. Lett. **56**, 949 (1990).

[22]J. Zhu, N. M. Johnson, and C. Herring, Phys. Rev. B **41**, 12 354 (1990).

[23]C. H. Seager and R. A. Anderson, Solid State Commun. **76**, 285 (1990).

[24]M. Capizzi and A. Mittiga, Appl. Phys. Lett. **50**, 918 (1987).

[25]J. T. Boreinstein, D. Angell, and J. W. Corbett, in *Characterization of the Structure and Chemistry of Defects in Materials,* edited by B. C. Larson, M. Ruhle, and D. N. Seidman, MRS Symposia Proceedings No. 138 (Materials Research Society, Pittsburgh, 1989), p. 209.

[26]C. H. Seager and R. A. Anderson, in *Characterization of the Structure and Chemistry of Defects in Materials* (Ref. 25), p. 209.

[27]J. P. Kalejs and S. Rajendran, Appl. Phys. Lett. **55**, 2763 (1989).

[28]D. Mathiot, Phys. Rev. B **40**, 5867 (1989).

[29]D. Mathiot, D. Ballutaud, P. de Mierry, and M. Aucouturier, in *Impurities, Defects and Diffusion in Semiconductors: Bulk and Layered Structures* (Ref. 6), p. 401.

[30]N. M. Johnson and C. Herring, in *Shallow Impurities in Semiconductors,* edited by B. Monemar, IOP Conf. Proc. No. 95 (Institute of Physics and Physical Society, London, 1988), p. 415.

[31]N. M. Johnson and M. D. Moyer, Appl. Phys. Lett. **46**, 787 (1985).

[32]N. M. Johnson, F. A. Ponce, R. A. Street, and J. Nemanich, Phys. Rev. B **35**, 4166 (1987).

[33]R. Rahbi, D. Mathiot, J. Chevallier, C. Grattepain, and R. M. Razeghi, in 6th Trieste Semiconductor Symposium on Hydrogen in Semiconductors: Bulk and Surface Properties [Physica B **170**, 135 (1991)].

[34]J. I. Pankove, R. O. Wance, and J. E. Berkeyheiser, Appl. Phys. Lett. **45**, 1100 (1984).

[35]G. G. DeLeo, W. B. Fowler, T. M. Sudol, and K. J. O'Brien, Phys. Rev. B **41**, 7581 (1990).

[36]S. J. Pearton, J. Electron. Mater. **14a**, 737 (1985).

[37]C. Herring and N. M. Johnson, Semiconductors and Semimetals Vol. 34 (Academic, New York, 1991), p. 224, and references therein.

[38]S. J. Pearton, J. W. Corbett, and J. T. Borenstein, in 6th Trieste Semiconductor Symposium on Hydrogen in Semiconductors: Bulk and Surface Properties [Physica B **170**, 85 (1991)], and references therein.

[39]A. Van Wieringen and N. Warmoltz, Physica **22**, 849 (1956).

[40]C. H. Seager and R. A. Anderson, Appl. Phys. Lett. **53**, 1181 (1988).

[41]K. J. Chang and D. J. Chadi, Phys. Rev. B **40**, 11 644 (1989).

[42]M. Stutzmann and M. Brandt, J. Appl. Phys. **68**, 1406 (1990).

[43]C. H. Seager, R. A. Anderson, and D. K. Brice, J. Appl. Phys. **68**, 3268 (1990).

[44]K. J. Chang and D. J. Chadi, Phys. Rev. Lett. **60**, 1422 (1988).

[45]K. J. Chang and D. J. Chadi, Phys. Rev. Lett. **62**, 937 (1989).

[46]P. Deak, L. C. Snyder, and J. W. Corbett, Phys. Rev. B **37**, 6887 (1988).

[47]C. P. Herrero, M. Stutzmann, A. Breitschwerdt, and P. V. Santos, Phys. Rev. B **41**, 1054 (1990).

[48]C. P. Herrero, M. Stutzmann, and A. Breitschwerdt, Phys. Rev. B. **43**, 1555 (1991).

[49]P. J. H. Denteneer, C. G. Van de Walle, Y. Bar-Yam, and S. T. Pantelides, Proceedings of the 15th International Conferences on Defects in Semiconductors, edited by G. Ferenczi, [Mater. Sci. Forum **38-41**, p. 979 (1989)].

[50]P. J. H. Denteneer, C. G. Van de Walle, and S. T. Pantelides, Phys. Rev. B **39**, 10 809 (1989).

[51]A. L. Endrös, W. Krühler, and J. Grobmaier, in 6th Trieste Semiconductor Symposium on Hydrogen in Semiconductors: Bulk and Surface Properties [Physica B **170**, 365 (1991)].